Highly charged ion X-rays from Electron–Cyclotron Resonance Ion Sources

P. Indelicato[a,*], S. Boucard[a], D.S. Covita[b], D. Gotta[c], A. Gruber[d], A. Hirtl[d], H. Fuhrmann[d], E.-O. Le Bigot[a], S. Schlesser[a], J.M.F. dos Santos[b], L.M. Simons[e], L. Stingelin[e], M. Trassinelli[a], J. Veloso[b], A. Wasser[e], J. Zmeskal[d]

[a]*Laboratoire Kastler Brossel, École Normale Supérieure, CNRS et Université Pierre et Marie Curie-Paris 6, Case 74, 4 place Jussieu, 75005 Paris, France*
[b]*Department of Physics, Coimbra University, P-3000 Coimbra, Portugal*
[c]*Institut für Kernphysik, Forschungszentrum Jülich, D-52425 Jülich, Germany*
[d]*Institut für Mittelenergiephysik, Austrian Academy of Science, Vienna*
[e]*Paul Scherrer Institut, Villigen PSI, CH5232 Villigen, Switzerland*

Available online 22 May 2007

Abstract

Radiation from the highly charged ions contained in the plasma of Electron–Cyclotron Resonance Ion Sources (ECRISs) constitutes a very bright source of X-rays. Because the ions have a relatively low kinetic energy ($\approx 1\,\text{eV}$) transitions can be very narrow, containing only a small Doppler broadening. We describe preliminary accurate measurements of two and three-electron ions with $Z = 16 - 18$. We show how these measurement can test sensitively many-body relativistic calculations or can be used as X-ray standards for precise measurements of X-ray transitions in exotic atoms.
© 2007 Published by Elsevier B.V.

PACS: 33.20.Rm; 36.10.−k; 29.25.Ni; 12.20.Fv

Keywords: X-ray spectroscopy; Exotic atoms; ECR ion source; Highly charged ions

1. Introduction

X-rays from X-ray tubes and targets excited by fluorescence have been used for a century to provide information on atomic and solid state structure, and as wavelength standards. Relativistic correlation effects and quantum-electrodynamics (QED) contributions have been the subject of numerous work that have lead after more than a quarter of a century of work to the publication of a new X-ray table, containing both all experimental values since the 1920s and advanced atomic calculations [1]. Yet all this considerable work does not allow for precise-enough tests of QED and relativistic effects in high fields, when the speed of the electron $Z\alpha c$ and the strength of the coupling with the nuclear charge $Z\alpha$ start to get large

(α is the fine structure constant, c is the speed of light and Z the atomic number). Lamb shift values have been extracted from experimental Kα line energies up to $Z = 100$ [2], but neither the theoretical accuracy nor the experimental one allows such data to make very good tests of QED in high-field. Moreover, because of the complex nature of inner-shell transitions in normal atoms, particularly when embedded in a solid matrix, their X-rays are not as suited as one would like as X-ray standards. In particular the lines are broad because of the Auger effect, deformed because of the outer-shell structure and multivacancies, and can be shifted because of chemical shifts and of their dependence on the excitation energy.

In contrast, few-electron ions or exotic atoms—atom in which a stable particle (by this we mean a particle that can live long enough to form an atom) is bound to a nucleus—can be used as high quality X-ray standards. Exotic atoms are in reality exotic highly charged ions, since the cascade

that follows the capture of the exotic particle by a normal atom leads to a series of ionizations. The mass of the exotic particle is so large (at the very least 200 times the mass of the electron for the lightest known exotic particle: the muon) that it can eject most bound electrons by Auger effect at the beginning of the cascade. Muons and pions can create fully stripped ions up to $Z = 18$, antiprotons can lead to fully stripped xenon. The X-rays that one observes, emitted at the end of the cascade are thus provided by an hydrogenic ion. The common feature of both highly charged ions and exotic atoms is thus that they are simple few-body systems, that can be calculated with good accuracy, have no or little broadening due to Auger effect. The use of such systems as X-ray standards has been proposed and demonstrated recently [3]. In the present work we consider X-rays emitted by two and three-electron heavy ions and by light exotic atoms. In Section 2, we will give a brief overview of recent experiments in the field of exotic atoms, of interest for the present discussion. In Section 3 we describe the experimental set-up common to both the exotic atoms and the highly charged ions, as used in the present work. The results are described in Section 4, and Section 5 is our conclusion.

2. X-ray standards for exotic atoms

In the last few years, the need of better X-ray standards has shown up in a series of experiments, performed at the Paul Scherrer Institute in Switzerland. The aim of these experiments was to make accurate measurements of the charged pion mass using pionic atoms, and of the strong interaction shift and broadening of the 1s level of pionic hydrogen. Pionic atoms are a specific example of exotic atoms. For light elements at least, the cascade following the capture of the particle, which is always much heavier than the electron, leads to a two body system, all the electrons being ejected by Auger effect.

The goal of these experiments was in one hand to provide a pion mass accurate to $\approx 2\,\mathrm{ppm}$, and in the other hand to measure the strong interaction broadening of the ground state level of pionic hydrogen of about 1 eV to an accuracy of less than 10 meV, an order of magnitude better than previous experiments [4]. Such an accuracy is required to obtain a meaningful test of Chiral Perturbation theory (ChPT) calculations [5,6], an effective field theory designed to perform Quantum Chromodynamics (QCD) calculation at low energy, a regime in which quark confinement precludes the use of perturbation theory in term of the QCD coupling constant. More recently the interest of doing similar measurements on pionic deuterium was pointed out [7] and the experiment was performed in the summer of 2006.

The previous measurements of the charged pion mass were performed by stopping a pion beam into a solid Mg target [8] and measuring the energy of a transition between two circular, high principal quantum number levels to avoid influence from strong interaction. The pionic

magnesium thus formed was able to recapture electrons from the solid, leading to a difficult analysis and to doubts on the reliability of the results [9–11]. A first experiment using a device called the Cyclotron Trap [12], designed to slow down beams of exotic particles and stop them in a nitrogen gas target, was then performed by our collaboration to remove this ambiguity [13]. The Kα spectrum of copper, in the fourth order of diffraction was used as a X-ray standard. This contributed noticeably to the final error budget. It was then decided to improve on this experiment by doing a direct comparison between the $5\mathrm{g} \rightarrow 4\mathrm{f}$ transitions in muonic oxygen, used as a X-ray standard, and pionic nitrogen, which are very close in energy. A new cyclotron trap (Cyclotron Trap II) was designed to optimize the capture of muons, which comes from the disintegration of the pions in the trap.

The strong interaction shift ($\approx 7\,\mathrm{eV}$) and broadening ($\approx 1\,\mathrm{eV}$) in pionic hydrogen are obtained by measuring the energy and line shape of X-ray transitions feeding the atomic 1s state [14]. The energies of the X-rays in question are 2.436, 2.886 and 3.043 keV for the $2\mathrm{p} \rightarrow 1\mathrm{s}$, $3\mathrm{p} \rightarrow 1\mathrm{s}$ and $4\mathrm{p} \rightarrow 1\mathrm{s}$ transitions, respectively. In order to attain the desired accuracy, a characterization of the spectrometer was in order, using narrow lines of energy close to those three pionic lines, and of width negligible compared to the best Bragg crystals energy resolution. It rapidly appeared that pionic or muonic X-rays where not up to the task, because of the very low counting rate that could be achieved. It was thus decided to look at highly charged heavy ion as an alternative method to obtain X-ray standards.

It was found that the so-called relativistic M1 transition $1\mathrm{s}2\mathrm{s}\ ^3\mathrm{S}_1 \rightarrow 1\mathrm{s}^2\ ^1\mathrm{S}_0$ (it has exactly 0 probability in a non-relativistic model) of sulfur, chlorine and argon had the exact energy required. Moreover their natural width of a few neV was completely negligible. It was also found that the magnetic field configuration of the improved cyclotron trap was perfect to turn it into a high-performance Electron–Cyclotron Resonance ion source (ECRIS). A single observation of X-ray transitions in helium-like argon had been performed at that time [15], and it was clear from the formation mechanism of the different charge states that the M1 transition X-ray emission should be very bright in a high-performance source [16]. A specific set of polar pieces and a permanent-magnet hexapole were constructed to enable to turn the cyclotron trap II into an electron–cyclotron resonance ion trap (ECRIT) [17]. This device has a very high magnetic field mirror ratio along its axis to improve the electron confinement, leading to very high-performances with a relatively modest frequency for the microwave (6.4 GHz) driving the electron–cyclotron resonance. The name ECRIT rather than ECRIS stems from the fact that our aim was to improve X-ray emission from the plasma inside the source, not to extract intense ion beams.

Here we provide a preliminary account of a new measurement of the $1\mathrm{s}2\mathrm{s}2\mathrm{p}\ ^2\mathrm{P}_J \rightarrow 1\mathrm{s}^2 2\mathrm{s}\ ^2\mathrm{S}_{1/2}$ transitions

in lithium-like sulfur, chlorine and argon, as an example of the accuracy that can be reached when combining the ECRIT with a high-performance spectrometer.

3. Experimental set-up

The experiment uses a Bragg spectrometer in Johann mounting [18] and was equipped with spherically bent silicon or quartz crystals having a diameter of 100 mm and a thickness of 0.3 or 0.2 mm, respectively. They were mounted by optical contact on glass lenses of ultimate quality. The curvature radius R_C of the bent crystals is $R_C \approx 2982$ mm and varies between individual crystals. These radii have been recently individually measured to the required accuracy. For these parameters, bent crystal theory predicts a negligible influence of the bending process on the crystal's rocking curve [19].

The experiment (Fig. 2) is composed of three parts:

- The ECRIT consists of a superconducting split coil magnet, which together with special iron inserts, provides the mirror field configuration, an Advanced ECR source—Updated version (AECRU-U) style permanent hexapole magnet and a 6.4 GHz power regulated microwave emitter [20]. The mirror field parameters provide one of the highest mirror ratios for ECR sources with a value of 4.3 over the length of the plasma chamber. The plasma chamber is formed by a 0.4 mm thick stainless steel tube of inner diameter of 85 mm and a length of 265 mm axially limited by copper inserts. At the position of the hexapole gap the stainless steel tube is perforated by a series of 2.5 mm diameter holes allowing for radial pumping in addition to axial pumping. The microwave high frequency power is introduced directly to the plasma chamber with waveguides exhibiting a small angle to the axis. In this way
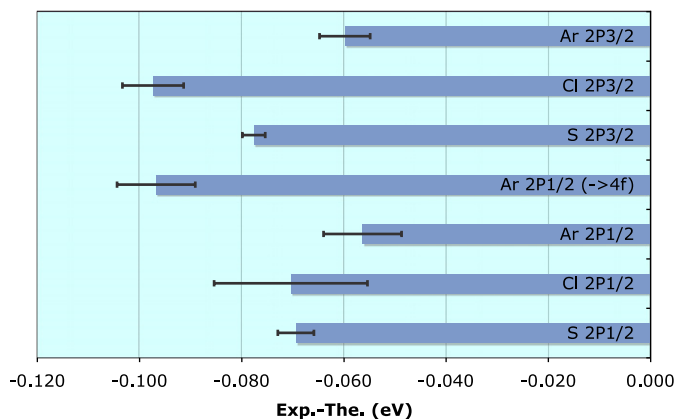
the path of the X-rays was at no point cut by any obstacle which could distort the shape of the response function. An extraction voltage of 2 kV had been routinely applied at the side opposite to the crystal spectrometer. The total ion current was measured as a control for a stable operation. More details on the ECRIT can be found in Refs. [17,21].

A reference pressure (without plasma) of 1.7×10^{-7} mbar was achieved. Gas filling was supplied radially by UHV precision leak valves through the gaps in the open structure hexapole. The gas composition was routinely surveyed with a quadrupole mass spectrometer. For an optimized plasma source a drastic increase of the number of energetic electrons was discovered which required the use of a cleaning magnet installed at a distance of 1 m in front of the crystal.

- A silicon(1 1 1) as well as a quartz(1 0 $\bar{1}$) crystal were investigated, which had been recently applied for measuring pionic hydrogen transitions [22]. The Bragg angles Θ_B, corresponding to the M1 transition of helium-like argon with an energy of 3.104 keV, are $\Theta_B = 36.68°$ for the quartz and $\Theta_B = 39.57°$ for the silicon crystal. The crystals were installed at a distance of 2330 mm from the centre of the ECRIT resulting in a position of the plasma about 500 mm outside the Rowland circle.
- A Charged Coupled Device (CCD) pixel detector with a pixel size of 40 μm × 40 μm and an energy resolution of 140 eV at 3 keV was used to detect the X-rays [23]. The detector consisted of six chips with 600 × 600 pixels each resulting in a total height of 72 mm and a width of 48 mm. The distance of the CCD detector from the crystal could be changed remotely over a length of 86 mm without breaking the vacuum.

The CCD detector and the associated electronics were protected against light as well as the high frequency stray field by a 30 μm thick beryllium window installed in the vacuum tube in front of the CCD cryostat.

4. Results and discussion

With the ECR source 20 000 events were reached for the narrow M1 transition of helium-like Argon in about 30 min time to be compared with 5000 counts reached after 40 h with X-rays from pionic carbon formed when using methane gas. A total of about 10 h was needed, however, to determine the spectrometer's response function in sufficient detail including changes of the distance CCD detector-crystal (focal scans) and changing apertures in front of the crystals. A complete survey of all Kα transitions for ions from helium-like to 1+ was performed [24]. In the present paper, we will focus on a preliminary measurement of the energy difference between the lithium-like 1s2s2p $^2P_J \rightarrow$ 1s^{2}2s $^2S_{1/2}$ and the helium-like M1 transition, used as a reference. Preliminary results for He-like lines have been presented elsewhere [24,25]. For the

Fig. 1. Comparison between the MCDF calculations presented in the text and preliminary experimental results, for the energy of the 1s2s2p $^2P_J \rightarrow$ 1s^{2}2s $^2S_{1/2}$, $J = \frac{1}{2}, \frac{3}{2}$ transition in lithium-like sulfur, chlorine and argon. The experimental error bars represent only statistical uncertainty. The average observed-theoretical value difference is 0.072 eV. Correlation energy is calculated within the $n = 3$ active space, except for one case, denoted by 4f in which it has been extended to $n = 4$.

energy value of this line, we take recent results from Ref. [26], which includes all QED corrections known to date. A complete Monte-Carlo simulation of the spectrometer is performed, in order to provide the line profiles to be fitted [21,25]. An example of spectra, together with the fit, is presented in Fig. 3.

In order to interpret the results, which are of much better accuracy than all previous measurements, we have performed Multi-Configuration Dirac–Fock calculations. In this variational method the wave function is represented as a linear combination of Slater determinants (configurations). We use the program of Desclaux and Indelicato [27,28] that contains first and second order QED corrections, including self-energy screening. This code was used in an earlier calculation of all argon lines [16,29] needed to interpret spectra from an ECRIS [15]. Here we have expanded on this previous work, by adding all the configurations that can be generated from all single and double excitations up to the $n = 3$ shell. In one case we performed a calculation including all correlation up to the $n = 4$ shell. From that, we can deduce that our calculation is accurate to within 40 meV. The self-energy screening has been evaluated by two different methods, one based on the Welton approximation, and the other one based on the direct evaluation of the QED diagrams [30]. This show that we can expect an uncertainty around 40 meV from QED. The results of the calculation for one transition in Ar, and a comparison with the experimental value are presented in Table 1.

In Fig. 1 we present the difference of the preliminary experimental transition energies and the theoretical ones, together with statistical fitting uncertainties. One can see that, even though different crystals have been used, and three different elements have been measured, this differences

are very close. This show that our results are already rather reliable and our analysis essentially correct. The average difference of 0.072 eV can be explained by missing

Table 1

Theoretical contributions to the $1s2s2p\ ^2P_{1/2} \rightarrow 1s^22s\ ^2S_{1/2}$ transition in Li-like Ar (eV)

Contribution	$1s2s2p\ ^2P_{1/2}$	$1s^22s\ ^2S_{1/2}$	Transition
Coulomb	−6353.4545	−9468.1885	3114.734
Magnetic	0.1800	2.2029	−2.023
Retardation	0.0479	−0.0216	0.069
Higher-order ret.	0.0012	0.0002	0.001
Coul. + Breit Corr.	−0.6318	−1.4534	0.822(41)
S.E.	1.3797	2.5972	−1.218
Screen (Welton)	−0.0381	−0.1226	0.085
V11	−0.0938	−0.1732	0.079
V13	0.0003	0.0006	0.000
Second order QED	−0.0012	−0.0021	0.001
Recoil	0.0001	0.0002	0.000
Total	−6352.6103	−9465.1604	3112.550
Experiment			3112.453(8)
Obs.-Calc.			−0.097(8)(41)
SE Screen (Ref. [30])	−0.0313	−0.1530	0.122
Total	−6352.6035	−9465.1908	3112.587
Obs.-Calc.			−0.134 (8)(41)

Numbers in parentheses represent uncertainty on the last digits. Coulomb: Dirac–Fock Coulomb contribution. Magnetic, retardation: Dirac–Fock contribution from the magnetic and retarded part of the relativistic electron–electron interaction in the Breit approximation. Higher-order ret.: retardation corrections beyond Breit interaction. S.E.: one-loop self-energy. Screen (Welton): self-energy screening correction in the Welton approximation [31,32]. V11: vacuum polarization in the Uehling approximation (see e.g., Refs. [33,34]), V13 Wichmann and Kroll correction [33,35]. Second order QED: sum of all two-loop radiative corrections.
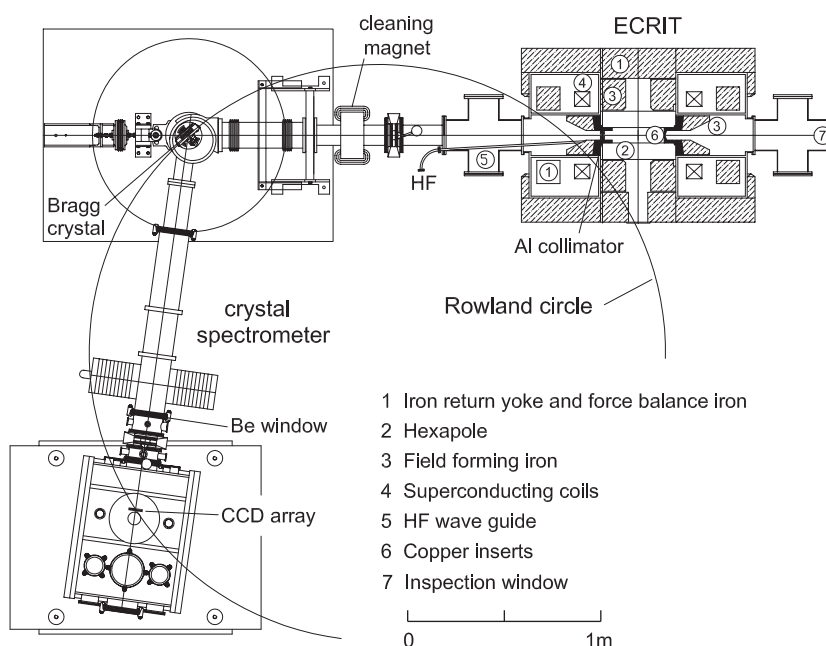

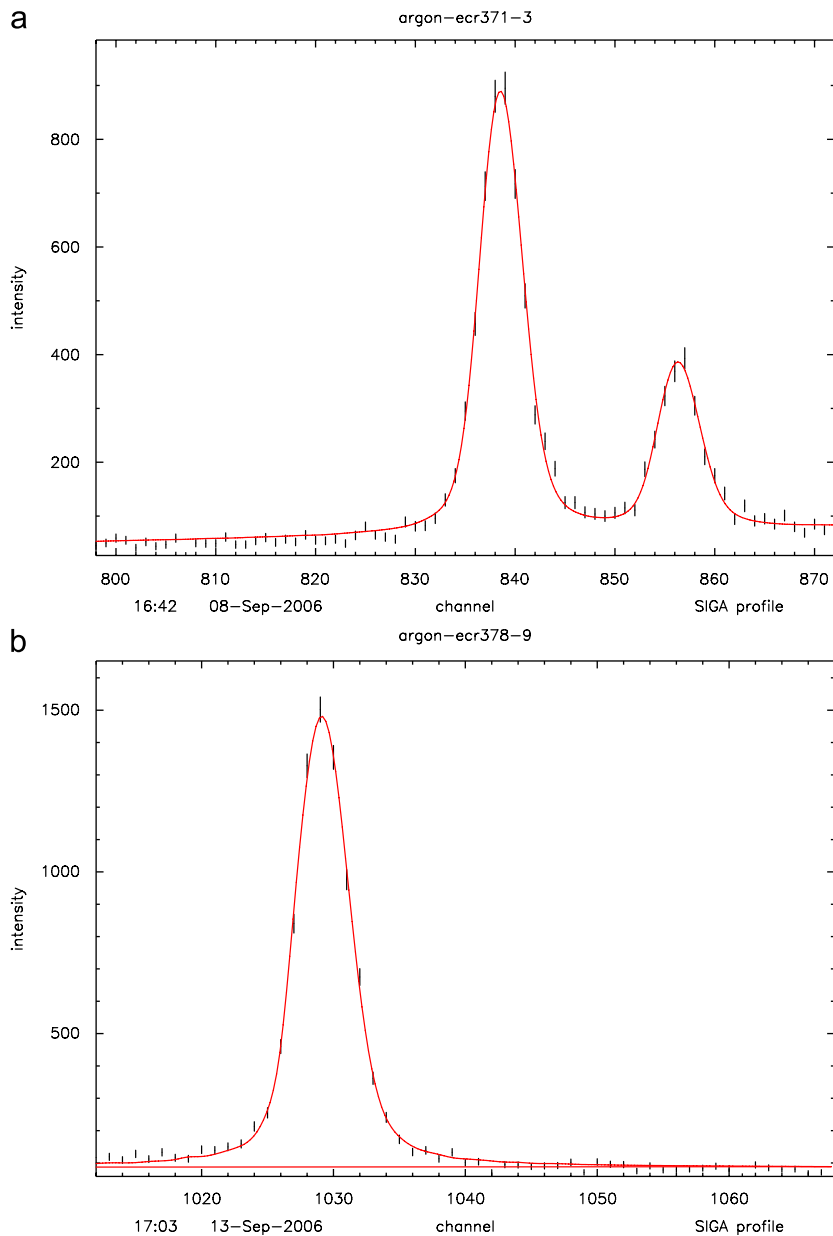Fig. 2. Set up of the PSI ECRIT together with the Bragg crystal spectrometer.

a

b

Fig. 3. The $1s2s2p\ ^2P_J \rightarrow 1s^22s\ ^2S_{1/2}$, $J = \frac{1}{2}, \frac{3}{2}$ transitions in lithium-like Ar (top) and the relativistic M1 transition ($1s2s\ ^3S_1 \rightarrow 1s^2\ ^1S_0$ in helium-like Ar (bottom, fitted with the profile discussed in the text).

correlation contribution, due to the limited basis set used, by the limitation of the QED corrections. One should also remember that the Li-like transitions that we are studying start from auto-ionizing levels. There should then be an Auger broadening, much smaller indeed than for the neutral case, because of the very small number of allowed decay channels. But there must be an Auger shift, of the same order of magnitude. The $1s2s2p\ ^2P_{3/2} \rightarrow 1s^22s\ ^2S_{1/2}$ transition has a radiative width of 66 meV and an Auger width of 6 meV, while for the $1s2s2p\ ^2P_{1/2} \rightarrow 1s^22s\ ^2S_{1/2}$ transition, these values are 57 and 65 meV, respectively [29]. To our knowledge Auger shifts have been calculated only for neutral atoms with a K, L or M hole [2,1].

5. Conclusion and outlook

We have presented preliminary values for the transition energies of Li-like of transition energy for Li-like ions, using the relativistic M1 transition from He-like ion as a reference. We get very accurate results, that compare quite well with theory. These measurements demonstrate the potential of the newly-developed ECRIT at PSI for studies of highly charged ions. They provide very interesting testing ground for relativistic many-body theory and QED, that cannot be matched by even the most accurate X-ray measurements on neutral atoms in solid targets.

Acknowledgements

References

[1] R. Deslattes, E. Kessler, Jr., P. Indelicato, L. de Billy, E. Lindroth, J. Anton, Rev. Mod. Phys. 75 (2003) 35, URL ⟨http://www.physics.nist.gov/PhysRefData/XrayTrans/index.html⟩.

[2] P. Indelicato, S. Boucard, E. Lindroth, Euro. Phys. J. D 3 (1998) 29.

[3] D.F. Anagnostopoulos, D. Gotta, P. Indelicato, L.M. Simons, Phys. Rev. Lett. 91 (2003) 240801.

[4] H.-C. Schröder, A. Badertscher, P.F.A. Goudsmit, M. Janousch, H.J. Leisi, E. Matsinos, D. Sigg, Z.G. Zhao, D. Chatellard, J.P. Egger, et al., Eur. Phys. J. C 21 (2001) 473.

[5] S. Weinberg, Physica A 96 (1979) 327.

[6] J. Gasser, M.A. Ivanov, E. Lipartia, M. Mojzis, A. Rusetsky, Eur. Phys. J. C 26 (2003) 13.

[7] U.-G. Meißner, U. Raha, A. Rusetsky, Euro. Phys. J. C 41 (2005) 213.

[8] B. Jeckelmann, T. Nakada, W. Beer, G. de Chambrier, O. Elsenhans, K.L. Giovanetti, P.F.A. Goudsmit, H.J. Leisi, A. Ruetschi, O. Piller, et al., Phys. Rev. Lett. 56 (1986) 1444.

[9] M. Daum, R. Frosch, D. Heter, M. Janousch, P.-R. Kettle, Phys. Lett. B 265 (1991) 425.

[10] B. Jeckelmann, P. Goudsmit, H. Leisi, Phys. Lett. B 335 (1994) 326.

[11] K. Assamagan, C. Brönnimann, M. Daum, H. Forrer, R. Frosch, P. Gheno, R. Horisberger, M. Janousch, P. Kettle, T. Spirig, et al., Phys. Rev. D 53 (1996) 6065.

[12] L.M. Simons, Hyp. Int. 81 (1993) 253.

[13] S. Lenz, G. Borchert, H. Gorke, D. Gotta, T. Siems, D. Anagnostopoulos, M. Augsburger, D. Chatellard, J. Egger, D. Belmiloud, et al., Phys. Lett. B 416 (1998) 50.

[14] D.F. Anagnostopoulos, S. Biri, V. Boisbourdain, M. Demeter, G. Borchert, J. Egger, H. Fuhrmann, D. Gotta, A. Gruber, M. Hennebach, et al., Nucl. Instr. and Meth. B 205 (2003) 9.

[15] G. Douysset, H. Khodja, A. Girard, J.P. Briand, Phys. Rev. E 61 (2000) 3015.

[16] M.C. Martins, A.M. Costa, J.P. Santos, P. Indelicato, F. Parente, J. Phys. B 34 (2001) 533.

[17] S. Biri, L. Simons, D. Hitz, Rev. Sci. Instrum. 71 (2000) 1116.

[18] H.H. Johann, Z. Phys. 69 (1931) 185.

[19] G. Hölzer, O. Werhahn, E. Förster, Cryst. Res. Technol. 33 (1998) 555.

[20] Z.Q. Xie, Rev. Sci. Instrum. 69 (1998) 625.

[21] D.F. Anagnostopoulos, S. Biri, D. Gotta, A. Gruber, P. Indelicato, B. Leoni, H. Fuhrmann, L.M. Simons, L. Stingelin, A. Wasser, et al., Nucl. Instr. and Meth. A 545 (2005) 217.

[22] D. Gotta, M. Hennebach, Y.W. Liu, V.E. Markushin, L.M. Simons, M. Cargnelli, H. Fuhrmann, M. Giersch, A. Gruber, A. Hirtl, et al., Phys. Scr. T 104 (2003) 94.

[23] N. Nelms, D.F. Anagnostopoulos, M. Augsburger, G. Borchert, D. Chatellard, M. Daum, J.P. Egger, D. Gotta, P. Hauser, P. Indelicato, et al., Nucl. Instr. and Meth. A 477 (2002) 461.

[24] M. Trassinelli, S. Biri, S. Boucard, D.S. Covita, D. Gotta, B. Leoni, A. Hirtl, P. Indelicato, E.-O. Le Bigot, J.M.F. dos Santos, et al., in: Electron Cyclotron Resonance Ion Sources: 16th International Workshop on ECR Ion Sources ECRIS'04, AIP, Berkeley, California (USA), 2005, vol. 749, pp. 81–84.

[25] M. Trassinelli, S. Boucard, D.S. Covita, D. Gotta, A. Hirtl, P. Indelicato, O.L. Bigot, J.M.F.d. Santos, L.M. Simons, L. Stingelin, J.F.C.A. Veloso, A. Wasser, J. Zmeskal, J. Phys.: Conf. Ser. 58 (2007) 129.

[26] A.N. Artemyev, V.M. Shabaev, V.A. Yerokhin, G. Plunien, G. Soff, Phys. Rev. A 71 (2005) 062104.

[27] J.P. Desclaux, in: E. Clementi (Ed.), Methods and Techniques in Computational Chemistry, STEF, Cagliary, 1993, vol. A: Small Systems of METTEC, p. 253, URL ⟨http://dirac.spectro.jussieu.fr/mcdf⟩.

[28] P. Indelicato, Phys. Rev. A 51 (1995) 1132.

[29] A.M. Costa, M.C. Martins, F. Parente, J.P. Santos, P. Indelicato, At. Data Nucl. Data Tables 79 (2001) 223.

[30] P. Indelicato, P.J. Mohr, Phys. Rev. A 63 (2001) 052507.

[31] P. Indelicato, O. Gorceix, J.P. Desclaux, J. Phys. B 20 (1987) 651.

[32] P. Indelicato, J.P. Desclaux, Phys. Rev. A 42 (1990) 5139.

[33] L.W. Fullerton, G.A. Rinker, Phys. Rev. A 13 (1976) 1283.

[34] S. Boucard, P. Indelicato, Eur. Phys. J. D 8 (2000) 59.

[35] E.H. Wichmann, N.M. Kroll, Phys. Rev. 101 (1956) 843.